Evaluation of a lower-powered analyser and sampling system for eddy-covariance measurements of nitrous oxide fluxes

Shannon E. Brown[1], Steve Sargent[2], Claudia Wagner-Riddle[1]

[1]School of Environmental Sciences, University of Guelph, Guelph, Ontario, Canada
5 [2]Campbell Scientific Inc., Logan, Utah, USA

Correspondence to: Shannon E. Brown (sbrown06@uoguelph.ca)

Abstract. Nitrous oxide (N_2O) fluxes measured using the eddy-covariance method capture the spatial and temporal heterogeneity of N_2O emissions. Most closed-path trace-gas analyzers for eddy-covariance measurements have large-volume, multi-pass absorption cells that necessitate high flow rates for ample frequency response, thus requiring high-power sample pumps. Other sampling system components, including rain caps, filters, dryers, and tubing can also degrade system frequency response. This field trial tested the performance of a closed-path eddy-covariance system for N_2O flux measurements with improvements to use less power while maintaining the frequency response. The new system consists of a thermoelectrically cooled tunable diode laser absorption spectrometer configured to measure both N_2O and carbon dioxide (CO_2). The system features a relatively small, single-pass sample cell (200 ml) that provides good frequency response with a lower-powered pump (~250 W). A new filterless intake removes particulates from the sample air stream with no additional mixing volume that could degrade frequency response. A single-tube dryer removes water vapor from the sample to avoid the need for density or spectroscopic corrections, while maintaining frequency response. This eddy-covariance system was collocated with a previous tunable diode laser absorption spectrometer model to compare N_2O and CO_2 flux measurements for two full growing seasons (May 2015 to October 2016) in a fertilized cornfield in Southern Ontario, Canada. Both spectrometers were placed outdoors at the base of the sampling tower demonstrating ruggedness for a range of environmental conditions (minimum to maximum daily temperature range: -26.1 to 31.6°C). The new system rarely required maintenance. An in situ frequency response test demonstrated that the cutoff frequency of the new system was better than the old system (3.5 Hz compared to 2.30 Hz), and similar to that of a closed-path CO_2 eddy-covariance system (4.05 Hz) using shorter tubing and no dryer that was also collocated at the site. Values of the

N$_2$O fluxes were similar between the two spectrometer systems (slope = 1.01, r^2 = 0.96); CO$_2$ fluxes as measured by the short-tubed eddy-covariance system and the two spectrometer systems correlated well (slope = 1.03, r^2 = 0.998). The new lower-powered tunable diode laser absorption spectrometer configuration with the filterless intake and single-tube dryer showed promise for deployment in remote areas.

1 Introduction

The concentration of N$_2$O in the atmosphere is rising and is of concern as N$_2$O has 298 times the global warming potential of CO$_2$ (IPCC, 2013). Agricultural systems contribute a significant proportion of total global N$_2$O emissions due to microbial soil processes (Davidson, 2009). The main drivers of microbial N$_2$O emissions are soil conditions (e.g., soil oxygen, carbon, and nitrogen levels), but distal drivers such as nitrogen fertilization, dry-wet, and freeze-thaw cycles also exert control and result in N$_2$O fluxes (F_{N2O}) that are highly variable in time ('hot moments') and in space ('hot spots') (Groffman et al., 2009; Molodovskaya, et al., 2012). This sporadic nature of F_{N2O} necessitates continuous measurements covering areas large enough to capture the spatial heterogeneity of the fluxes to sufficiently quantify total emissions from agricultural systems (Flechard et al., 2007; Jones et al., 2011; Shurpali et al., 2016). The eddy-covariance (EC) technique gives long-term, continuous, and spatially integrated measurements, which can fully capture F_{N2O}. Advances in technology for N$_2$O analyzers has increased the number of long-term N$_2$O measurement campaigns using EC methods (Mishurov and Kiely, 2010; Molodovskaya et al., 2012; Merbold et al., 2014; Huang et al., 2014; Rannik et al., 2015; Shurpali et al., 2016; Wang et al., 2016). However, the application has been limited to sites with high-quality power or short-term deployment. Locations with agricultural N$_2$O emissions are often rural areas where it may be impractical and expensive to install permanent power infrastructure for long-term F_{N2O} EC flux measurements.

Gas analyzers used in EC systems require fast responses to distinguish the high frequencies of concentration fluctuations (McBean, 1972; Leuning and Judd, 1996). High-frequency concentration

fluctuations can be attenuated by line averaging within the sample cell, as well as sample mixing within various system components, such as intake tubing, dryers, filters, and rain caps (Moore, 1986; Massman, 2000). Analyzer frequency response often represents a significant proportion of the total high-frequency losses (Horst, 1997; Kroon et al., 2010b), but these sampling-system components may

5   also significantly degrade system frequency response (Aubinet et al., 2016). Modern closed-path analyzers for CO_2 EC fluxes achieve high frequency response with low-power pumps by using small sample cells (6 or 16 ml) that operate near ambient pressure (Burba et al., 2010; Novick et al., 2013). The volume of sampling-system components is minimized to preserve the frequency response without excessive flow restriction that would increase power requirements for the pump, or exceed the range of

10   the sample-cell pressure sensor (Aubinet et al., 2016; Ma et al., 2017).

In contrast, all N_2O analyzers tested in a recent EC field intercomparison have large sample cells (~ 500 ml) that must operate at significantly reduced pressure (50 to 120 mb), necessitating high flow rates (12 to 17 L min^{-1}) (Rannik et al., 2015). The high flow rate and low pressure requires the use of a relatively

15   high-power pump (500 to 1000 W). Reducing the volume of the sample cell and sampling-system components is a means of maintaining good frequency response at a lower flow rate while reducing the power requirements of N_2O EC systems. Using a dryer on the intake line may degrade system frequency response, but can eliminate uncertainties associated with spectroscopic corrections for line broadening due to water vapor (Neftel et al., 2010) and density corrections (Webb et al., 1980). The typically high

20   sample flow rates require the use of multi-tube dryers to achieve an acceptable residual humidity. However, laminar flow within the dryer degrades system frequency response because air velocity varies from the center to the wall of the tube (Leuning and Judd, 1996), and multi-tube dryers can further degrade frequency response if the flow varies among the individual tubes. This problem cannot be overcome by simply increasing flow because a higher flow would require a larger dryer. Alternatively,

25   analyzers with smaller sample cells require lower sample flow, allowing the use of single-tube dryers and lower-powered pumps to achieve the frequency response required for EC measurements.

An upgraded version of a first-generation tunable diode laser absorption spectrometer (TDLAS) (Edwards et al., 2003) has recently been made commercially available (TGA200A, Campbell Scientific Inc., Logan, Utah, USA). The previous model was suitable for long-term N_2O flux measurements for a variety of agricultural and forested sites (Scanlon and Kiely, 2003; Pihlatie et al., 2005; Pattey et al.,

5   2006; Mishurov and Kiely, 2010; Molodovskaya et al., 2012). The upgraded model has been designed to reduce power consumption of EC measurement systems by reducing the volume of the sample cell. This was done without changing the path length, thereby preserving measurement precision. The smaller sample cell allows a lower flow rate, enabling the use of a single-tube dryer that maintains frequency response better than high-capacity, multi-tube dryers. Adapting a new vortex intake—

10 originally developed for use with a CO_2/H_2O EC analyzer (Ma et al., 2017)—to the N_2O analyzer should further improve the frequency response as this device removes particulates from the air stream without adding a significant mixing volume. The vortex intake has the additional advantage of not requiring a traditional filter that can clog over time, restricting flow to the analyzer, and requiring maintenance. This is an important aspect of EC system design for long-term studies because, as stated

15 by Nelson et al. (2004), all components need to be sufficiently rugged to withstand exposure to environmental conditions and run reliably for long time periods with minimal maintenance.

Cutoff frequencies are often used to characterize the frequency response of EC analyzers and systems (McBean, 1972; Nelson et al., 2004; Detto et al., 2011; Rannik et al., 2015) and for correcting flux

20 values for high-frequency losses (Moore, 1986; Horst, 1997; Aubinet et al., 2000; Massman, 2000; Massman and Lee, 2002). Determining frequency response using field-measured cospectra (Aubinet et al., 2000; Ibrom et al., 2007) is challenging for N_2O EC systems as this requires a strong concentration signal occurring simultaneously with environmental conditions appropriate for scaling with temperature spectra. Direct characterizations are more appropriate for N_2O analyzers since emission events may

25 occur for only a few days in a year, reducing the likelihood of ideal conditions for cospectral analyses. Similarly, evaluating system lag times of closed-path N_2O analyzers used for EC flux processing with the standard cross-correlation method requires a strong signal (Kroon et al., 2010b; Neftel et al., 2010).

Directly measuring lag times will give a better estimate of the tube delay for periods with low N_2O signals.

5   We present the first field trial of a new TDLAS with an optimized sampling system, operating at lower flow rates with a lower-powered pump. Continuous F_{N2O} measurements are presented over two growing seasons for an agricultural site in a cold climate. The system was evaluated for overall performance of the instrument in terms of ease of operation, data quality, and suitability for EC measurements. N_2O fluxes measured by the new TDLAS were compared to those measured by the previous generation

10   TDLAS and CO_2 fluxes (F_{CO2}) were compared to fluxes measured by a short-tubed CO_2 analyzer. A novel method for determining EC system frequency response and lag time was conducted in situ to determine the analyzer frequency response under field operating conditions.

2 Methods

2.1 Study Site

15   Flux measurements took place at the Elora Research Station, Elora, Ontario, Canada (43.3° 27.8' N 80.24° 20.4' W) from May 2015 to October 2016 as a part of a four-plot flux-gradient study on the effect of nitrogen fertilizer management practices on F_{N2O}. The four 4-ha plots were located within a larger 30-ha aerodynamically homogeneous and flat field (Fig. 1a) under the same crop management practices. The soil at the site was a Guelph silt loam (fine loamy, mixed, mesic *Glossoboric Hapludalf*).

20   Corn was planted 10 May 2015 and again on 5 May 2016. Urea fertilizer was broadcast-applied at the time of planting in both years to the plot where instrumentation was set up (Fig. 1a). Corn grew to a maximum height of approximately 2.5 m each summer. Harvest for 2015 started on 27 October and completion was delayed due to rain until 2 November. The field was tilled immediately afterwards, leaving a bare-soil surface from 2 November 2015 to 30 May 2016 when the corn emerged. Harvest in

25   2016 occurred on 7 October. The field plot was located 400 m from an Environment Canada weather station that measured supporting variables of mean wind direction, air temperature, pressure, and precipitation.

2.2 Eddy Covariance Measurements

An EC system (CPEC200, Campbell Scientific Inc., Logan, Utah, USA) was installed in the southeast corner of the 4-ha plot (Fig. 1a, 1c) and was comprised of a sonic anemometer (CSAT3A) to measure three-dimensional wind and sonic temperature, a closed-path infrared gas analyzer (EC155) to measure mixing ratios of CO_2 and H_2O, and a datalogger (CR3000). The sonic anemometer was oriented towards the predominant wind direction (270°) (Fig. 1b). Two TDLAS were added to this system (TGA100A and TGA200A, Campbell Scientific Inc., Logan, Utah, USA) (see details below). Each measured mixing ratios of N_2O and CO_2. The analyzers include temperature-controlled, weatherproof cases that allowed them to be placed on two cinder blocks set on the ground at the base of the tower (Fig. 1c). Details on the operation of each gas analyzer are given below. The EC measurements were made at a height of 2.0 m when the surface was bare; the intakes and sonic anemometer were raised to 1.75 m above the canopy top throughout the growing seasons. Data from the sonic anemometer and all three analyzers were recorded at a sampling rate of 10 Hz. Each gas analyzer included a user-configurable digital filter set for a 5 Hz cutoff frequency to avoid aliasing.

2.3 Gas Analyzers

The operating principles of the TDLAS used can be found in Edwards et al. (2003) and Wagner-Riddle et al. (2005). Briefly, a temperature-controlled laser emits a beam at an absorption wavelength of the gas species of interest. This beam is split and directed through the sample cell as well as a reference cell supplied with a known reference gas. The laser wavelength is swept across an individual absorption line by adjusting the laser current. This produces the absorption spectrum, measured by detectors at the ends of the reference and sample cells. The mixing ratio in the sample cell is calculated from the ratio of the spectral absorbance of the reference and sample cells. Both TDLAS are capable of simultaneous measurement of multiple trace gases on separate absorption lines (dual-ramp mode). For periods during this study, the analyzers were set to measure the absorption of N_2O and $^{13}CO_2$.

Table 1 lists the equipment and measurement mode used for each analyzer through the measurement campaign. Operating configurations of N_2O analyzers used in Rannik et al. (2015) are given for

comparison. The analyzers included enclosure temperature controllers to maintain temperatures of 20°C in winter and 40°C in summer. Flow from the reference gas cylinders was set at 10 ml min^{-1}. Analyzer calibrations were performed shortly after the initial installation and repeated each time a reference cylinder was replaced. Additional information on calibration and correction of $^{13}CO_2$ to total CO_2 can

5 be found in the Supplementary Materials.

The "legacy" TDLAS (TGA100A, manufactured in 2005, hereafter referred to as TDLAS-LN) used a cryogenically cooled, lead salt diode laser operating at 83.5 K and 2243.11 cm^{-1} (N_2O) and 2343.585 cm^{-1} (CO_2). The TDLAS-LN required twice-weekly filling of the laser dewar with liquid nitrogen. This

10 analyzer was operated in a dual-ramp mode measuring both N_2O and CO_2 throughout the measurement campaign, following a typical air-sampling configuration for EC measurements (Fig. 1d) (see also: Mammarella et al., 2010; Mishurov and Kiely, 2010; Molodovskaya, 2012; Rannik et al., 2015). Air was sampled through a 6 ml rain-shielded intake (part number 17882, Campbell Scientific, Inc., Logan, Utah, USA) and a dryer assembly (PD1000, Campbell Scientific, Inc., Logan, Utah, USA), which

15 included a 2 μm polypropylene filter element in a low-volume, high-flow filter holder, and a multi-tube dryer (200-tube, 1.2 m Nafion^{TM} dryer element; Perma Pure, Lakewood, New Jersey, USA). A tee fitting and needle valves split the flow between dryer purge (3 L min^{-1}) and sample flow directed to the analyzer (14.5 L min^{-1}) (Fig. 1d). Tubing between the intake, dryer assembly, and the analyzer was 4.3 mm ID Synflex^{TM} tubing. The total length of tubing (plus dryer) from the intake to the analyzer was 6 m

20 from 10 May 2015 to 8 July 2015, at which time the tubing length was increased to 10 m to accommodate the increase in canopy height. A 950 W rotary vane pump (RB0021, Busch Vacuum Technics, Inc., Boisbriand, Quebec, Canada) was connected to the analyzer using ~50 m of 25.4 mm ID PVC suction hose (Tigerflex K100, Kuri Tec, Brantford, Ontario, Canada), to draw air through the analyzer and the dryer purge (Fig. 1d). The volume of the sample cell of TDLAS-LN was 480 ml. This

25 setup is similar to the TGA100A used by Rannik et al. (2015), although for the present study the original filter holder (Gelman 1235, Pall Corp.), included as part of the dryer assembly, was updated to a newer design (part number 20553, Campbell Scientific, Inc., Logan, Utah, USA) with lower volume

(5 ml compared to 20 ml). Filter elements were replaced approximately every 2 weeks. The nominal sample cell pressure was 58 mb throughout the measurement campaign.

The new N_2O analyzer (TGA200A, hereafter referred to as TDLAS-TE) was similar to the TDLAS-LN with two major upgrades: a smaller-diameter sample cell and a room-temperature laser. It used a distributed feedback interband cascade laser (DFB ICL, nanoplus Nanosystems and Technologies GmbH, Gerbrunn, Germany) that was cooled thermoelectrically as opposed to with liquid nitrogen. The laser temperature was set to -1°C and the laser current was tuned to measure N_2O at 2237.7 cm^{-1} and CO_2 at 2237.3 cm^{-1} from 10 May 2015 to 29 May 2015, when the laser was configured to measure N_2O at 2235.5 cm^{-1} to assess performance of the laser in single-ramp mode for approximately 2 months. On 31 July 2015, the laser was switched back to dual-ramp mode until 31 March 2016. On this date, a new N_2O-only laser was installed in the TDLAS-TE. This laser operated at -2.4°C at 2208.6 cm^{-1}.

The sample cell of TDLAS-TE has a similar length (1.5 m) compared to the TDLAS-LN, but a smaller inner diameter (12.7 mm compared to 18.8 mm). The smaller inner diameter gives the newer sample cell a volume of 200 ml, a reduction of 280 ml from the original size. From 10 May 2015 to 22 June 2015 the TDLAS-TE sampling system (intake assembly, dryer, and pump) was similar to that of the TDLAS-LN. The TDLAS-TE sampling system was replaced on 24 June 2015 with a new prototype design including a vortex intake and single-tube dryer (Fig. 1e), optimized to take advantage of the smaller sample-cell volume. The intake assembly and filter were replaced with a vortex intake that removes particulates without a traditional filter (U.S. Patent No. 9,217,692). The vortex intake was adapted for this application by extending the length of the sample tube (2.2 mm ID stainless steel) to 1.1 m, and by providing a separate high-capacity filter (Numatics PXB-02, ASCO Numatics, Florham Park, New Jersey, USA) and diaphragm pump (E163-11-120, Parker-Hannifin, Inc. Hollis, NH) for the bypass flow. On 24 December 2015 this pump was replaced by one designed for long-term continuous use (L061B-11, Parker-Hannifin, Inc. Hollis, New Hampshire, USA). The multi-tube dryer was replaced with a prototype design using a single Nafion® tube (2.2 mm ID, 7.3 m long TT-110, Perma Pure LLC, Lakewood, New Jersey, USA). The tube was housed in a large-diameter (25.4 mm) flexible

shell to allow it to be purged in reflux mode with little pressure drop. A needle valve at the outlet of the dryer controlled the sample-flow rate to 3.5 L min^{-1}. The total length of the intake assembly and dryer was 9.1 m. A short (0.1 m) tube (4.3 mm ID Synflex^{TM}) connected the needle valve to the analyzer inlet. A lower-powered (250 W) dry scroll pump (nXDS6i, Edwards Ltd., West Sussex, United

5 Kingdom) pulled the sample air through the intake assembly, dryer, and analyzer via approximately 50 m of 25.4 mm ID PVC suction hose (Tigerflex K100, Kuri Tec, Brantford, Ontario, Canada) (Fig. 1e). The nominal sample cell pressure was 59 mb at the start of the measurement campaign and set to 35 mb after the new sampling system was installed on 24 June 2015.

10 CO_2 and H_2O fluxes were measured with a closed-path EC system (CPEC200) that included the gas analyzer (EC155), sonic anemometer (CSAT3A), as well as the sample pump, enclosures, and mounting hardware. Details on the EC155 analyzer can be found in Novick et al. (2013). This CPEC200 system was configured with the manufacturer's valve module for automatic zero and span, as well as a scrub module to supply dry, CO_2-free air for setting zero on the analyzer (see details in Supplementary

15 Materials). The system was configured to automatically set the analyzer to zero and CO_2 span daily at 1:00 AM. The EC155 was reconfigured on 10 February 2016 with the production version of the vortex intake/sample cell prototype that was tested by Ma et al. (2017). Nominal flow settings of 8 L min^{-1} total flow, with 6 L min^{-1} through the EC155 sample cell and 2 L min^{-1} for the vortex bypass, were used.

20 **2.4 Frequency Response Test**

The impulse response method (Sargent, 2012) was used in situ to measure the frequency response of each EC system, and derive the tube delay (t_{del}), cutoff frequency (f_c), and effective time constant (τ_e). Briefly, this method entails injecting an impulse of high N_2O and CO_2 concentration into the sample air stream. Measuring the response to this impulse and taking the Fourier transform of this result gives the

25 frequency response. This gives a conservative estimate of the frequency response of the system, as any attenuation of high frequencies caused by the test method are included in the system frequency response.

The impulse responses were measured in situ for each analyzer by injecting high-concentration (2500 ppm N_2O and 30000 ppm CO_2) gas directly into the intake with a fast-acting solenoid valve (VHS micro dispense valve, The Lee Co., Westbrook, Connecticut, USA) driven with a spike-and-hold driver
5   (part number IECX0501350AA, The Lee Co.) every 10 s, as controlled by a datalogger. For the TDLAS-TE and EC155, which were equipped with the vortex intake, the dispense valve nozzle was inserted into the rain cap end for a test of the complete system. The TDLAS-LN used a rain cap that did not permit this direct injection. This rain cap was removed and replaced with a small adapter to mount the valve. The dispense valve was driven open for less than 5 ms for each pulse. For the N_2O analyzers,
10   frequency response was measured at various pressures, including the standard operating pressure (TDLAS-LN: 29, 38, 45, and 58 mb; TDLAS-TE: 28, 30, 35, and 43 mb). These pressures were achieved by adjusting the needle valve that sets the sample flow. The EC155 frequency response was measured with the production version of the vortex-intake assembly. The concentration data and the voltages to the solenoid valve were recorded at 20 Hz for 20 min per test.

The impulse response was calculated by subtracting the average ambient background N_2O or CO_2 concentrations from the data, overlaying the multiple 10 s periods, and then taking an average of the responses. The t_{del} was calculated as the delay from the valve-open signal to the peak of the impulse response, minus processing time for the analyzer (750, 372, and 800 ms, respectively, for TDLAS-LN,
20   TDLAS-TE, and EC155). This tube delay represents the physical travel time through the sampling system and into the analyzer sample cell.

The frequency response was calculated as the normalized amplitude of the Fourier transform of the
25   impulse response. The f_c was determined graphically as the frequency at which the frequency response reached a value of $1/\sqrt{2}$. Following common practice, we compared this frequency response to a linear, first-order system (Moore, 1986, Horst, 1997; Massman, 2000, Massman and Lee, 2002, Ibrom, 2007).

This transfer function is often related to electronic circuits, but it also describes transfer function of an ideal mixing volume (Horst, 1997). The amplitude of the transfer function (T_{FR}) is:

$$T_{FR} = \frac{1}{\sqrt{1 + \left(\frac{f}{f_c}\right)^2}} \tag{1}$$

Alternately, the transfer function may be parametrized by an effective time constant (τ_e), calculated using:

$$\tau_e = \frac{1}{2\pi f_c} \tag{2}$$

Theoretical residence times (τ_{res}) of the analyzer sample cells were calculated based on the sample-cell volume, pressure, and flow rates from Table 1. Theoretical cutoff frequencies ($f_{c,t}$) and corresponding theoretical effective time constants ($\tau_{e,t}$) were calculated from τ_{res} using different models for multi-pass and single-pass sample cells. Multi-pass sample cells, which tend to be relatively short for a given volume with low length to diameter ratios, are often modelled with the assumption of perfect mixing ($\tau_{e,t} = \tau_{res}$) (Nelson, et al., 2004). In contrast, the EC155, TDLAS-LN, and TDLAS-TE have higher length to diameter ratios and have relatively long, narrow sample cells. For these analyzers the theoretical frequency response is modelled assuming no mixing in the sample cell, which is analogous to line averaging in a sonic anemometer when the sonic path is aligned with the wind vector. The amplitude transfer function for line averaging is (Mitsuta, 1966):

$$T_{LA} = \sqrt{\sin^2\left(\pi\tau_{res}f\right)/(\pi\tau_{res}f)^2} \tag{3}$$

This transfer function has an approximate cutoff frequency:

$$f_{c,t} = \frac{2.78}{2\pi\tau_{res}} \tag{4}$$

The corresponding effective time constant from eq. 2 is:

$$\tau_{e,t} = \frac{1}{2\pi f_{c,t}} = \frac{\tau_{res}}{2.78} \tag{5}$$

2.5 Flux Calculations

Fluxes were calculated as the covariance between fluctuations of the scalar concentration (*s*) and the vertical wind velocity (*w*):

$$F_s = \overline{w's'} \qquad (6)$$

5   where *s* is the mixing ratio of either N_2O or CO_2.

Fluxes were calculated for 30 min time intervals in Matlab^{TM} using modifications to functions from Sturm et al. (2012). The vertical wind was despiked and then rotated using a double rotation (Aubinet et al., 2012; Kaimal and Finnigan, 1994). The high-frequency concentration data for all analyzers was
10   despiked and filtered according to instrument diagnostic codes. Concentration measurements from both N_2O analyzers were filtered for periods of equipment maintenance or malfunction. All concentrations measured by TDLAS-TE and the EC155 were linearly detrended. Concentration data from TDLAS-LN were linearly detrended until winter of 2016 when the concentration signal periodically indicated optical fringing of the laser. A Chebyshev filter was used to detrend and remove the artificial low-frequency
15   fluctuations for those 30 min periods. The 30 min flux values were filtered for low wind-speed conditions (friction velocity (u_*) < 0.1 m·s^{-1}) and wind direction of 60 to 120° (shadow of instrument tower). Vibrations from strong winds against the side of TDLAS-LN caused increased concentration noise. This occurred during periods when the field was bare and mean wind speeds were greater than 5 m s^{-1} from 200° to 360°. Data from these periods were filtered out. Flux data from TDLAS-TE were not
20   affected by the strong winds as it was sheltered by TDLAS-LN for southwest to northerly wind directions, and data with winds against the side of TDLAS-TE were already filtered out due to tower interference (Fig. 1).

Lag times (t_l) for analyzers measuring CO_2 concentration (TDLAS-TE when operated under dual-ramp
25   mode; TDLAS-LN and EC155) were calculated using cross-correlation such that t_l was the time delay that maximized the covariance between the concentration and *w* signals. CO_2 concentrations were used for the t_l calculation as the N_2O signal was too weak for cross-correlations for the majority of time periods, as was also observed by Kroon et al. (2010a). This was determined on a day-by-day basis as the

conditions that affected concentration signal delays (e.g., pump performance, filter clogging) remained relatively consistent on a daily time scale. For the daily lag value, t_l was calculated for individual 30 min periods per day with the strongest F_{CO2} as determined from raw 30 min flux values. An average of six lag times for each analyzer was used for a given day. Lag times ranged from 0.5 to 1.0 s for the

5   TDLAS-TE and 0.6 to 1.2 s for the TDLAS-LN; t_l for the EC155 was consistent at 0.1 s. Processing delays in the sonic anemometer and the gas analyzers were subtracted from these lag times to calculate tube delays for comparison with t_{del} derived from the frequency response test. Values for t_l derived from t_{del} and sonic processing delays were used for periods when the TDLAS-TE was setup to measure only N_2O concentrations.

The τ_e derived from the frequency response test was used to calculate corrections for high-frequency losses using the simplified formula given by Horst (1997):

$$T_r = \frac{1}{1+\left(2\pi n_m \frac{U}{z}\tau_e\right)^\alpha} \tag{7}$$

where U is the mean wind speed, z is the measurement height, n_m and α are constants determined from

15   the idealized spectra of Kaimal et al. (1972) using values for unstable and stable conditions as presented by Horst (1997).

2.6 Flux Comparisons

Half-hourly F_{N2O} and F_{CO2} obtained with the two TDLAS were compared over the whole measurement

20   period, and F_{CO2} from both TDLAS were also compared to the EC155. Agreement was evaluated based on r^2 and slope of the linear regression between values from the different analyzers. Cumulative F_{N2O} over the measurement period for each TDLAS were calculated. No gap filling was applied to the time series, so totals do not represent absolute emissions for this site. Emissions were accumulated using only 30 min F_{N2O} when data were available from both analyzers and converted from ng N_2O-N m^{-2} s^{-1} to

25   g N_2O-N ha^{-1}.

Random errors of each of the individual 30 min F_{N2O} (δ_F) as measured by the TDLAS-LN and TDLAS-LE, were calculated using the filtering method of Salesky et al. (2012). This method was preferred over those requiring an estimate of the turbulent integral time scale (e.g., Finkelstein and Sims, 2001) as time scales can vary depending on definition (Dias et al., 2004). Salesky et al. (2012) showed that error

5   estimates from the filtering method compared well to those using integral scales. Briefly, this method entailed repeatedly applying filters of increasing width (Δt) to the high frequency instantaneous fluxes from each 30 min period. Standard deviations of each set of filtered data were fit to $\Delta t^{-1/2}$. These successive power-law fits were then fit to the entire averaging period to estimate the 30 min δ_F. Propagation of δ_F was then used to calculate the confidence intervals ($p = 0.05$) of the total cumulative

10   F_{N2O} for the TDLAS-TE and TDLAS-LN time series.

Flux detection limits (δF) were calculated using the method described in Blomquist et al. (2010) and Yang et al. (2016) where the detection limit is calculated using the instrument noise and the variability of the concentration signal:

15   $$\delta F = \frac{2\sigma_w}{\sqrt{T_f}}\left[\sigma_{C_a}^2\, \tau_{wc} + \frac{\varphi_{C_n}}{4}\right]^{1/2} \tag{8}$$

such that σ_w is the standard deviation of w, T_f is the flux-averaging period, $\sigma_{C_a}^2$ is the ambient variance of the concentration signal, τ_{wc} is the integral timescale for the ambient concentration variance, and φ_{Cn} is the band-limited analyzer noise. The φ_{Cn} were calculated as the mean of the variance spectra from 1 to 5 Hz. Values of $\sigma_{C_a}^2$ were calculated as the second point of the autocovariance of the concentration

20   signal (Yang et al. 2016). Blomquist et al. (2010) estimated τ_{wc} using the peak frequency of the variance cospectrum. Peak frequencies here were modelled via the equation given in Horst (1997).

3 Results

3.1 N$_2$O Fluxes and Data Coverage

25   Measurements of fluxes covered two growing seasons (May to Oct in 2015 and 2016), one post-harvest period (November to December 2015), winter (January to February 2016), and early spring (March to

April 2016). Winter was classified as the period when nighttime temperatures were consistently below freezing. Fig. 2 displays the mean daily air temperatures and precipitation for 2015 and 2016. Mean hourly air temperatures ranged from -26.1°C to 31.6°C. Winter of 2016 was on average 3°C warmer than 30-year normals and the maximum snow depth was relatively low at 8 cm. Precipitation totals were

5   close to 30-year normal values for both years; however, May of 2015 received only 17 mm of rainfall until May 31, which was considerably less than the normal amount of 89 mm. Rainfall was lower than normal in May, June and July of 2016 with monthly totals 50% lower than the 30-year monthly normals.

10   Non-gap-filled mean daily N_2O fluxes obtained with the TDLAS are shown in Fig. 3. One major N_2O flux event occurred in 2015, one day after the first significant rainfall after planting and fertilizer application (8 June 2015 and 9 June 2015, day of year (DOY) 159 and 160 in Fig. 3a). The daily mean 30 min F_{N2O} values for this event as measured by both analyzers were 600 ng N_2O-N m^{-2} s^{-1} with the 30 min fluxes during the daytime exceeding 800 ng N_2O-N m^{-2} s^{-1} for several hours. Two subsequent post-

15   fertilizer flux events occurred after rainfall on 16 June 2015 and 28 June 2015 (DOY 167, 179, Fig. 2a) and were smaller in magnitude with daily average fluxes of 100 ng N_2O-N m^{-2} s^{-1}. Throughout the remainder of the growing season of 2015 and post-harvest period of 2015, mean daily fluxes were small and varied between -10 to 10 ng N_2O-N m^{-2} s^{-1}. The warmer-than-average winter in 2016 limited flux emissions from freeze-thaw processes that have been typically observed at this site (Furon et al., 2008;

20   Risk et al., 2013; Abalos et al., 2015; Congreves et al., 2017; Wagner-Riddle et al., 2017) with average daily fluxes ranging from 0 to 30 ng N_2O-N m^{-2} s^{-1} (Fig. 3b). The abnormally dry spring in 2016 prevented any significant N_2O flux events associated with fertilizer application. Peak post-fertilizer daily flux values from 5 May 2016 to 13 June 2016 (DOY 126 to 165 in Fig. 3c) averaged 25 ng N_2O-N m^{-2} s^{-1}. Daily flux values in the summer period of 2016 remained small (~ 5 ng N_2O-N m^{-2} s^{-1}, Fig. 3c)

25   but predominantly positive throughout the summer.

Both analyzers performed well throughout the measurement period and maintenance requirements were minimal for both. Of the total number of 30 min periods for the whole measurement period, 44% of the

30 min flux values were filtered out due to low friction velocity, wind direction and footprint criteria, warnings from the sonic anemometer from precipitation, disruption from field operations, and power outages. Further filtering based on analyzer operation and diagnostics resulted in an additional removal of 16% (TDLAS-TE) and 28% (TDLAS-LN) of the fluxes due to equipment failure and periods of

5 equipment reconfiguration. Longer data gaps occurred mostly for the TDLAS-LN due to pump malfunction, a faulty power supply, and an electronic module failure. Data outage for the TDLAS-TE in September 2015 was due to failure of the diaphragm pump providing bypass flow for the vortex intake before a model designed for long-term use was installed. Intermittent periods of data losses for both TDLAS also occurred when the enclosure temperature settings prevented the heaters from maintaining a

10 constant temperature. This occurred at night during spring and fall periods when differences between daytime and nighttime temperatures were greatest, and midday in the summer months when air temperatures exceeded 30°C.

3.2 Frequency Response Test

15 The in situ frequency response test characterized the frequency response and tube delay for the three analyzers under the operating pressures tested. Impulse response peaks were at minimum 5 ppm (N_2O) and 600 ppm (CO_2) above ambient concentrations. The peaks were consistent throughout each of the 20 min tests with an average coefficient of variation of 1.8%. The precision of the impulse responses was further improved by averaging the 120 peaks in each test. Frequency-response curves for each analyzer

20 obtained at the nominal cell pressure (Table 1) are given in Fig. 4. The frequency-response curve for the EC155 drops steeply at 5 Hz as expected due to its digital anti-aliasing filter. The effect of the digital filters is not distinctly visible for the N_2O analyzers, but all three analyzers have little or no response at or near the Nyquist frequency (10 Hz), giving confidence that the frequency response curves are not contaminated by aliasing. Table 2 contains the corresponding cutoff frequencies and effective time

25 constants. The EC155 showed the best frequency response ($f_c = 4.05$ Hz and $\tau_e = 39$ ms) for CO_2 (Table 2). The frequency response to N_2O of TDLAS-TE was nearly as good as the EC155 ($f_c = 3.5$ Hz, $\tau_e = 48$ ms), while TDLAS-LN showed lower frequency response ($f_c = 2.3$ Hz and $\tau_e = 69$ ms). TDLAS-LN

measured both N_2O and CO_2 during the frequency response test; results for CO_2 were identical to those for N_2O (data not shown). These measured f_c were used in equation 1 to calculate T_{FR}, which are shown for comparison in Fig. 4. Spectral losses (equation 7) calculated with the f_c were on average 5% of the measured flux for the TLDAS-TE and 7% for the TDLAS-LN. All measured f_c values were lower than

5 the best-case theoretical cutoff frequencies ($f_{c,t}$) calculated from τ_{res} (Table 2), indicating some attenuation of high frequencies in the sampling system components and sample cells, as expected. Frequency responses for both N_2O analyzers were tested at a range of pressures as varying field conditions can cause pressures to drift with pump performance and, in the case of TDLAS-LN, filter clogging. The TDLAS-LN f_c increased significantly with pressure (1.1 Hz at 29 mb to 2.3 Hz at 58 mb),

10 whereas the response of the TDLAS-TE showed less variation (3.1 Hz at 28 mb to 3.65 Hz at 43 mb) (data not shown). Response times calculated using measured cospectra are included in the Supplementary Materials.

Tube delays determined from the impulse responses at the nominal cell pressure for the three analyzers

15 are given in Table 2. As expected, the EC155 had the shortest t_{del} at 100 ms. The tube delay of TDLAS-TE was longer (578 ms) due to the greater tubing length and lower flow rate. The tube delay for TDLAS-LN was longest at 720 ms, despite its higher flow rate, due to the larger volumes for its tubing, filter, and dryer. Tube delays for the N_2O analyzers over the range of operating pressures showed a decrease in t_{del} with increasing cell pressure (Fig. 5). Decreases in flow rate with pressure for TDLAS-

20 LN acted to increase t_{del} to a greater degree than for the TDLAS-TE. Tube delays determined from the cross-correlation of CO_2 with w ranged from 650 to 1450 ms for TDLAS-LN and 550 to 1050 ms for TDLAS-TE, and were consistent with those determined from the impulse response (Fig. 5).

3.4 Flux Comparison

25 Comparison of F_{N2O} showed similar values for both TDLAS on short and long time scales. Fig. 6a shows the agreement between 30 min F_{N2O} values measured by each analyzer ($r^2 = 0.97$, slope = 1.01). The majority (86%) of 30 min N_2O fluxes were small and below 20 ng N_2O-N m^{-2} s^{-1}. The general

correspondence between the TDLAS-LN and TDLAS-TE flux values remained for the small flux values (Fig. 6b). Scatter in the low F_{N2O} (Fig. 6b) was related to instrument noise. Both analyzers showed excellent agreement with the CO_2 fluxes measured using the EC155. The slope and correlation coefficient of the linear regression between the EC155 and TDLAS-TE were, respectively, 1.03 and 0.998 (Fig. 6c). Similarly, the slope and correlation coefficient of the linear regression between the EC155 and TDLAS-LN were 1.03 and 0.998 (data not shown).

Figure 7 shows the mean variance spectra of the N_2O signals from each TDLAS analyser for a period of 10 days where no N_2O fluxes were observed (29 June 2016 to 9 July 2016). The variance spectra of both analyzers were dominated by instrument noise as N_2O emissions were at background levels. Values of φ_{Cn} were 0.28 $ppb^2\,Hz^{-1}$ for the TDLAS-TE and 0.22 $ppb^2\,Hz^{-1}$ for the TDLAS-LN. When considering only instrument noise, detection limits with mean conditions of $U = 3.5$ m s^{-1}, $z = 4$ m, and $\sigma_w = 0.5$ m s^{-1} were 6.6 ng N_2O-N m^{-2}s^{-1} for the TDLAS-TE and 5.2 ng N_2O-N m^{-2}s^{-1} for the TDLAS-LN. Incorporating signal noise increased δF_{N2O} to 9.9 ng N_2O-N m^{-2}s^{-1} for the TDLAS-TE and 19.6 ng N_2O-N m^{-2}s^{-1} for the TDLAS-N. Despite the lower instrument noise, concentration signals of the TLDAS-LN were less steady than the TLDAS-TE during the period evaluated ($\sigma_{C_a}^2$ of 0.27 ppb^2 and 0.042 ppb^2, respectively).

Emissions were accumulated over the measurement period to evaluate the long-term comparison of the total F_{N2O} (Fig. 8). From planting of 2015 to harvest of 2016, TDLAS-TE measured total emissions of 1247 ± 11.3 g N_2O-N ha^{-1} and TDLAS-LN measured 1272 ± 9.3 g N_2O-N ha^{-1}, where uncertainties are the propagated random errors.

4 Discussion

Both N_2O analyzers were well suited for the long-term and continuous measurement of F_{N2O} that are required to fully capture the temporal dynamics of N_2O emissions (Savage et al., 2014; Shurpali et al., 2016). Both operated continuously for over 1.5 years through the various environmental conditions

encountered in southern Ontario. Data gaps were caused by problems with sample pumps, a power supply failure, and from reconfigurations for the intercomparison experiment, (e.g., frequency response testing, swapping lasers, and reconfiguring the sampling systems). Disregarding these time periods, data coverage of 56% was typical for EC measurements at that site after typical EC filtering for rainy

5   periods, low wind speeds, and wind direction (Santos et al., 2011; Brown et al., 2013). Further steps can be taken to reduce data losses attributable to the TDLAS operation, including adjusting the analyzer's internal-temperature setpoint more frequently (seasonally to monthly), and protecting the analyzer from strong winds. A simple baffle the height of the analyzer (0.55 m) along the side of the analyzer facing the mean wind direction would provide sufficient shelter from strong winds ($U > 5$ m s^{-1}).

The older TDLAS-LN system required periodic maintenance including liquid nitrogen fills (twice weekly), replacing filter elements (twice monthly), and changing pump oil (monthly). The TDLAS-TE system with the vortex intake and dry scroll pump required no routine maintenance. The TDLAS-TE also operated using less power for the sample pump than the TDLAS-LN (250 W versus 950 W). The

15   ruggedness and low maintenance of TDLAS-TE through all seasons showed the suitability of the analyzer for capturing post-fertilizer and freeze-thaw emissions.

The TDLAS-TE system, with smaller sample-cell volume, single-tube dryer, and vortex intake had better frequency response ($f_c = 3.5$ Hz) than the TDLAS-LN system ($f_c = 2.30$ Hz), while operating at

20   lower flow rates (3.5 compared to 14.5 L min^{-1}) and with lower sample pump power consumption. The TDLAS-TE cutoff frequency of 3.5 Hz was only slightly lower than that of the short-tubed EC155 closed-path analyzer ($f_c = 4.05$ Hz). The frequency response of the TDLAS-TE system was affected less by changes in pressure and flow rate than the TDLAS-LN which helped to maintain constancy of f_c with the slight variations in pressure that occur during long-term field operations. The frequency response of

25   TDLAS-LN was still adequate for EC measurements (McBean, 1972, Eugster et al., 2007). Rannik et al. (2015) reported EC system time constants calculated from cospectra ($\tau_{e,s}$) for several N$_2$O analyzers, which are summarized in Table 2. The same model N$_2$O analyzer (TGA100A) with a similar sampling system at similar flow (17 L min^{-1}) and pressure (50 mb) had a $\tau_{e,s}$ of 120 ms. The lower τ_e in this study

(69 ms) is likely related to the shorter tube and newer lower-volume filter holder as compared to the higher-volume filter holder used in the Rannik et al. (2015) study, or discrepancies between our direct frequency response assessment compared to deriving τ_e from cospectral analyses. Rannik et al. (2015) found a disagreement of almost a factor of two in the N_2O and CO_2 time constants for a system that measured both gases, opting to use the value measured for CO_2 for spectral corrections of both gases. However, it is difficult to directly compare the absolute values of the frequency-response τ_e with the commonly used cospectra method (Detto et al., 2011; Peltola et al., 2014; Rannik et al., 2015; Aubinet et al., 2016). The cospectral method is highly dependent on the adherence of the spectra to similarity scaling, and is also affected by sensor separation and by imperfect synchronization of the scalar with vertical wind. The frequency-response test provided a direct assessment of sampling system response times, as it eliminates the possibility of response times being affected by artefacts of the temperature or w spectra.

Analyzer sample cell and sampling system design both have an impact on system frequency response. Multi-pass sample cells tend to be much shorter but with larger diameters compared to single-pass sample cells; therefore, the air flow tends to behave as a mixing volume. Measured τ_e for analyzers with multi-pass sampling cells are generally greater than the τ_{res} of the sample cell. Nelson, et al. (2004) directly measured the frequency response of an analyzer with a multi-pass sample cell using an exponential fit to measurements of a step change in concentration. Their τ_e of 63 ms was slightly greater than the theoretical time constant (τ_{res} = 54 ms). Neftel et al. (2010) measured the time constant for an EC system with a similar sample cell using the same step-change technique. The measured τ_e of 400 ms was more than twice the theoretical time constant (τ_{res} = 175 ms) of the sample cell, likely due to the long tube (30 m) and other sampling components. Single-pass sample cells, which tend to be long and narrow, have less mixing as the air flows through the cell, giving them a theoretical advantage of a factor of 2.78 compared to multi-pass sample cells. The TDLAS-TE τ_e was within 15% of this theoretical $\tau_{e,t}$, indicating near ideal performance in the sample cell and sampling system. The EC155 τ_e was a factor of two larger than the theoretical $\tau_{e,t}$. This is likely due to mixing in the sample cell, which

has a length/diameter ratio of 15, compared to 110 for the TDLAS-TE. TDLAS-LN has a diameter/length ratio of 75, suggesting its performance should also approach the ideal. However, the TDLAS-LN τ_e was 40% greater than $\tau_{e,t}$, compared to 15% for TDLAS-TE. This additional frequency response degradation was most likely caused by attenuation in the multi-tube dryer. Ratios of $\tau_e/\tau_{e,t}$ from similar analyzers operating without driers (Table 2) were comparable to those of the TDLAS-LN and TDLAS-TE systems, although not directly as spectral calculations of τ_e were used in that study.

Operating the N_2O systems with driers prevented uncertainties from spectroscopic and density corrections. Improper application of the WPL corrections, as well as variations in flux processing steps, can affect flux values (Aubinet et al. 2012; Mammarella et al., 2016). For fluxes close to zero, WPL corrections for fluctuations in water vapor can be greater than the value of the scalar flux, and uncertainty of the correction can be of similar magnitude to the small fluxes (Detto et al., 2011). Line-broadening caused by moisture in the sample can also cause significant errors in F_{N2O} (Neftel et al., 2010).

Lag times can be difficult to determine using cross-correlation methods on data with weak signals, which is often the case for N_2O (Pihlatie et al., 2005; Neftel et al., 2010). Inaccurate lag times can lead to underestimations of flux values. The t_{del} from the impulse response tests corresponded well with the t_l obtained for CO_2 using the cross-correlation method. The t_{del} measured with the impulse response method reduced uncertainty in the N_2O lag times used in the flux processing in the absence of a CO_2 signal. This approach is useful for long-term studies measuring agricultural N_2O fluxes when signals are too weak for automatic covariance maximization and when variations in operating conditions preclude the use of a constant lag value. Tube-delay of the TDLAS-TE (0.6 s at 35 mb) was lower than that of the TDLAS-LN (0.8 s at 58 mb), showing the improved transit time of the upgraded intake system. These values were comparable to tube delay values of analyzers operated without driers (Rannik et al., 2015), showing how the TDLAS systems used here (with driers) could be optimized for fast response, while also avoiding corrections associated with lack of air drying.

5 Conclusions

The field trial of the new TDLAS-TE analyzer with the optimized sampling system consisting of a vortex intake, single-tube drier and lower-power pump demonstrated the ability of this analyzer to operate continuously through several field seasons with minimal maintenance with the frequency response needed for EC measurements. The frequency response was comparable to that of a short-tubed CO_2 EC system, and was better than published reports of N_2O EC systems operating without driers.

The legacy TDLAS-LN analyzer presented a lower cut-off frequency and higher tube delay than the TDLAS-TE and EC155, but showed improvement over previous reports due to the use of a shorter intake tube and a lower volume filter holder. The 30 min F_{CO2} and F_{N2O} values measured by the TDLAS systems compared well; F_{CO2} values measured by these systems were also comparable with the EC155.

More studies of long-term, multi-season N_2O fluxes are needed to improve global estimates of agricultural N_2O emissions (Reay et al., 2012; Wagner-Riddle et al., 2017). The optimal performance combined with its lower power and low maintenance requirements make the TDLAS-TE suitable for N_2O flux measurements under rugged field conditions in remote or rural areas where power quality can be a concern.

References

Abalos, D., Brown, S. E., Vanderzaag, A. C., Gordon, R. J., Dunfield, K. E., and Wagner- Riddle, C.: Micrometeorological measurements over 3 years reveal differences in N_2O emissions between annual and perennial crops, Global Change Biology., 3, 1244-1255, 2015.

Aubinet, M., Lilian , J., Loustau, D., De Ligne, A., Chopin, H., Cousin, J., Chauvin, N., Decarpenterie, T., and Gross, P.: Dimensioning IRGA gas sampling systems: laboratory and field experiments, Atmos. Meas. Tech., 9, 1361-1367, doi:10.5194/amt-9-1361, 2016.

Aubinet, M., Vesala, T., and Papale, D. (Eds.): Eddy Covariance: A Practical Guide to Measurement and Data Analysis. Springer, 2012.

Aubinet, M., Grelle, A., Ibrom, A., Rannik, Ü., Moncrieff, J., Foken, T., Kowalski, A., Martin, P.,
5 Berbigier, P., Bernhofer, C., Clement, R., Elbers, J., Granier, A., Grünwald, T., Morgenstern, K., Pilegaard, K., Rebmann, C., Snijders, W., Valentini, R., and Vesala, T.: Estimates of the annual net carbon and water exchange of forests: The EUROFLUX methodology, Advances in Ecological Research, 30, 113-175, doi:10.1016/S0065-2504(08)60018-5, 2000.

10 Blomquist, B., Huebert, B., Fairall, C., and Faloona, I.: Determining the sea-air flux of dimethylsulfide by eddy correlation using mass spectrometry, Atmospheric Measurement Techniques, 3, 1-20, 2010.

Brown, S. E., Warland, J. S., Santos, E., Wagner-Riddle, C., Staebler, R. M., and Wilton, M.: Estimating a Lagrangian length scale using measurements of CO_2 in a plant canopy, Boundary-Layer
15 Meteorology, 147, 83-102, 2013.

Burba, G.: Eddy covariance method for scientific, industrial, agricultural and regulatory applications: A field book on measuring ecosystem gas exchange and areal emission rates, LI-Cor Biosciences, Lincoln, NE, USA, 331 pp., 2013.
20
Burba, G. G., McDermittt, D. K., Anderson, D. J., Furtaw, M. D., and Eckles, R.: Novel design of an enclosed CO_2/H_2O gas analyser for eddy covariance flux measurements, Tellus B, 62, 5, 743-748, 2010.

Congreves, K., Brown, S., Nemeth, D., Dunfield, K., and Wagner-Riddle, C.: Differences in field-scale
25 N_2O flux linked to crop reside removal under two tillage systems in cold climates, Global Change Biology Bioenergy, doi:10.1111/gcbb.12354, 2017.

Davidson, E. A.: The contribution of manure and fertilizer nitrogen to atmospheric nitrous oxide since 1860, Nature Geosciences, 2, 9, 659–662, 2009.

Detto, M., Verfaillie, J., Anderson, F., Xu, L., and Baldocchi, D.: Comparing laser-based open- and closed-path gas analyzers to measure methane fluxes using the eddy covariance method, Agricultural and Forest Meteorology, 151, 10, 1312-1324, 2011.

Dias N., Chamecki M., Kan A., and Okawa C.: A study of spectra, structure and correlation functions and their implications for the stationarity of surface-layer turbulence, Boundary-Layer Meteorology, 110(2), 165–189, 2004.

Edwards, G., Thurtell, G., Kidd, G., Dias, G., and Wagner-Riddle, C.: A diode laser based gas monitor suitable for measurement of trace gas exchange using micrometeorological techniques, Agricultural and Forest Meteorology, 115, 71-89, 2003.

Eugster, W., Zeyer, K., Zeeman, M., Minchna, P., Zingg, A., Buchmann, N., and Emmengger, L.: Methodical study of nitrous oxide eddy covariance measurements using quantum cascade laser spectrometery over a Swiss forest, Biogeosciences, 4, 927-939, 2007.

Finkelstein, P. L., and Sims, P. F.: Sampling error in eddy correlation flux measurements, Journal of Geophysical Research, 106, D4, 3503-3509, 2001.

Flechard, C., Ambus, P., Skiba, U., Rees, R., Hensen, A., Van Amstel, A., van den Pol-van Dasselaar, A., Soussana, J.-F., Jones, M., Clifton-Brown, J., Raschi, A., Horvath, L., Neftel, A., Jocher, M., Ammann, C., Leifeld, J., Fuhrer, J., Calanca, PL, Thalman, E., Pilegaard, K., Marco, C., Campbell, C., Nemitz, E., Hargreaves, K., Levy, P., Ball, B., Jones, S., van de Bulk, W., Groot, T., Blom, M., Domingues, R., Kasper, G., Allard, V., Ceschia, E., Cellier, P., Laville, P., Henault, C., Bizouard, F., Abdalla, M., Williams, M., Baronti, S., Berretti, F., and Grosz, B.: Effects of climate and management

intensity on nitrous oxide emissions in grassland systems across Europe, Agriculture, Ecosystems & Environment, 121, 135-152, 2007.

Furon, A. C., Wagner-Riddle, C., Smith, C. R., and Warland, J. S.: Wavelet analysis of wintertime and spring thaw CO_2 and N_2O fluxes from agricultural fields. Agricultural and Forest Meteorology, 148, 1305-1317, 2008.

Groffman, P.M., Butterbach-Bahl, K., Fulwieler, R.W., Gold, A.J., Morse, J.L., Stander, E.K., Tague, C., Tonitto, C., and Vidon, P.: Challenges to incorporating spatially and temporally explicit phenomena (hotspots and hot moments) in denitrification models. Biogeochemistry 93:49-77, 2009.

Horst, T. W.: A simple formula for attenuation of eddy fluxes measured with first-order- response scalar sensors, Boundary-Layer Meteorology, 82, 2, 219-233, 1997.

Huang, H., Wang, J., Hui, D., Miller, D. R., Bhattarai, S., Dennis, S., Smart, D., Sammis, T., and Reddy, K. C.: Nitrous oxide emissions from a commercial cornfield (zea mays) measured using the eddy covariance technique. Atmospheric Chemistry and Physics, 14, 23, 12839-12854, 2014.

Ibrom, A., Dellwik, E., Flyvbjerg, H., Jensen, N.O., and Pilegaard, K.: Strong low-pass filtering effects on water vapor flux measurements with closed-path eddy correlation systems, Agricultural and Forest Meteorology, 147, 3-4, 140-156, 2007.

IPCC, Climate Change: The Physical Science Basis. Contribution of Working Group I to the Fifth Assessment Report of the Intergovernmental Panel on Climate Change. Cambridge University Press, Cambridge, United Kingdom and New York, USA, 2013.

Jones, S. K., Famulari, D., Marco, C. F. D., Nemitz, E., Skiba, U. M., Rees, R. M., and Sutton, M. A.: Nitrous oxide emissions from managed grassland: a comparison of eddy covariance and static chamber measurements, Atmospheric Measurement Technology, 4, 2179-2194, 2011.

5   Kaimal, J. and Finnigan, J. J.: Atmospheric Boundary Layer Flows: Their Structure and Measurement. Oxford University Press, New York, USA, 304 pp., 1994.

Kaimal, J. C., Wyngaard, J. C., Izumi, Y., and Cote, O. R.: Spectral characteristics of surface-layer turbulence, Quarterly Journal of the Royal Meteorological Society, 98, 417, 563-589, 1972.

Kroon, P., Hensen, A., Jonker, H., Ouwersloot, H., Vermeulen, A., and Bosveld, F.: Uncertainties in eddy covariance flux measurements assessed from CH_4 and N_2O observations, Agricultural and Forest Meteorology, 150, 6, 806-816, 2010a.

15   Kroon, P., Schuitmaker, A., Jonker, H., Tummers, M., Hensen, A., and Bosveld, F.: An evaluation by laser Doppler anemometry of the correction algorithm based on Kaimal cospectra for high frequency losses of EC flux measurements of CH_4 and N_2O, Agricultural and Forest Meteorology, 150, 6, 794-805, 2010b.

20   Leuning, R. and Judd, M. J.: The relative merits of open- and closed-path analysers for measurement of eddy fluxes, Global Change Biology, 2, 3, 241-253, 1996.

Ma, J., Zha, T., Jia, X., Sargent, S., Burgon, R., Bourque, C. P.-A., Zhou, X., Liu, P., Bai, Y., and Wu, Y.: An eddy-covariance system with an innovative vortex intake for measuring carbon dioxide and 25   water fluxes of ecosystems, Atmos. Meas. Tech., 10, 1259-1267, doi:10.5194/amt-10-1259-2017, 2017.

Mammarella, I., Werle, P., Pihlatie, M., Eugster, W., Haapanala, S., Kiese, R., Markkanen, T., Rannik, U., and Vesala, T.: A case study of eddy covariance flux of N_2O measured within forest ecosystems: quality control and flux error analysis, Biogeosciences, 7, 2, 427-440, 2010.

5   Massman, W. J.: A simple method for estimating frequency response corrections for eddy covariance systems, Agricultural and Forest Meteorology, 104, 185-198, 2000.

Massman, W. J. and Lee, X.: Eddy covariance flux corrections and uncertainties in long-term studies of carbon and energy exchanges, Agricultural and Forest Meteorology, 113, 1-4,121-144, 2002.

McBean, G. A.: Instrument requirements for eddy correlation measurements. Journal of Applied Meteorology, 11, 1078-1084, 1972.

Merbold, L., Eugster, W., Stieger, J., Zahniser, M., Nelson, D., and Buchmann, N.: Greenhouse gas
15   budget (CO_2, CH_4, and N_2O) of intensively managed grassland following restoration, Global Change Biology, 20, 6, 1913-1928, 2014.

Mishurov, M. and Kiely, G.: Nitrous oxide flux dynamics of grassland undergoing afforestation, Agriculture, Ecosystems & Environment, 139, 1-2, 59-65, 2010

Mitsuta, Y.: Sonic Anemometer-Thermometer for General Use, Journal of the Meteorological Society of Japan, 44, 1, 12-23, 1966.

Molodovskaya, M., Singurindy, O., Richards, B. K., Warland, J., Johnson, M. J., and
25   Steenhuis, T. S.: Temporal Variability of Nitrous Oxide from Fertilized Croplands: Hot Moment Analysis, Soil Sci. Soc. Am. J., 76, 1728-1740, 2012.

Moore, C. J.: Frequency response corrections for eddy correlation systems, Boundary Layer Meteorology, 37, 1, 17-35, 1986.

Neftel, A., Ammann, C., Fischer, C., Spirig, C., Conen, F., Emmenegger, L., Tuzson, B., and Wahlen, S.: N_2O exchange over managed grassland: Application of a quantum cascade laser spectrometer for micrometeorological flux measurements, Agricultural and Forest Meteorology, 150, 6, 775-785, 2010.

Nelson, D. D., McManus, B., Urbanski, S., Herndon, S., and Zahniser, M. S.: High precision measurements of atmospheric nitrous oxide and methane using thermoelectrically cooled mid-infrared quantum cascade lasers and detectors, Spectrochimica Acta Part A: Molecular and Biomolecular Spectroscopy, 60, 14, 3325-3335, 2004.

Novick, K., Walker, J., Chan, W., Schmidt, A., Sobek, C., and Vose, J.: Eddy covariance measurements with a new fast-response, enclosed-path analyzer: Spectral characteristics and cross-system comparisons, Agricultural and Forest Meteorology, 181, 17-32, 2013.

Pattey, E., Strachan, I., Desjardins, R., Edwards, G., Dow, D., and MacPherson, J.: Application of a tunable diode laser to the measurement of CH_4 and N_2O fluxes from field to landscape scale using several micrometeorological techniques, Agricultural and Forest Meteorology, 136, 3-4, 222-236, 2006.

Pihlatie, M., Rinne, J., Ambus, P., Pilegaard, K., Dorsey, J. R., Rannik, U., Markkanen, T., Launiainen, S., and Vesala, T.: Nitrous oxide emissions from a beech forest floor measured by eddy covariance and soil enclosure techniques, Biogeosciences, 2, 4, 377-387, 2005.

Rannik, U., Haapanala, S., Shurpali, N. J., Mammarella, I., Lind, S., Hyvönen, N., Peltola, O., Zahniser, M., Martikainen, P. J., and Vesala, T.: Intercomparison of fast response commercial gas analysers for nitrous oxide flux measurements under field conditions, Biogeosciences, 12, 2, 415-432, 2015.

Reay, D. S., Davidson, E. A., Smith, K. A., Smith, P., Melilo, J. M., Dentener, F., and Crutzen, P. J. Global agriculture and nitrous oxide emissions, Nature Climate Change, 2, 410-416, 2012.

Risk, N., Snider, D., and Wagner-Riddle, C.: Mechanisms leading to enhanced soil nitrous oxide fluxes induced by freeze-thaw cycles, Canadian Journal of Soil Science, 93, 4, 401-414, 2013.

Salesky, S., Chamecki, M., and Dias, N.: Estimating the random error in eddy-covariance based fluxes and other turbulence statistics: The filtering method. Boundary-Layer Meteorology, 114, 113-135, 2012.

Santos, E., Wagner-Riddle, C., and Warland, J.: Applying Lagrangian dispersion analysis to infer carbon dioxide and latent heat fluxes in a corn canopy, Agricultural and Forest Meteorology, 151, 620-632, 2011.

Sargent, S. Quantifying frequency response of a low-power, closed-path CO_2 and H_2O eddy-covariance system. Technical report, Campbell Scientific Inc, Logan, Utah, U.S., 10 pp., 2012.

Savage, K., Phillips, R. and Davidson, E.: High temporal frequency measurements of greenhouse gas emissions from soils, Biogeosciences, 11, 2709-2720, 2014.

Scanlon, T. M. and Kiely, G.: Ecosystem-scale measurements of nitrous oxide fluxes for an intensely grazed, fertilized grassland, Geophysical Research Letters, 30, 16, 1-4, 2003.

Shurpali, N. J., Rannik, U., Jokinen, S., Lind, S., Biasi, C., Mammarella, I., Peltola, O., Pihlatie, M., Hyvonen, N., Raty, M., Haapanala, S., Zahniser, M., Virkajarvi, P., Vesala, T., and Martikainen, P. J.: Neglecting diurnal variations leads to uncertainties in terrestrial nitrous oxide emissions, Scientific Reports, 6, doi:10.1038/srep25739, 2016.

Sturm, P., Eugster, W., and Knohl, A.: Eddy covariance measurements of CO_2 isotopologues with a quantum cascade laser absorption spectrometer, Agricultural and Forest Meteorology, 152, 73-82, 2012.

Yang, M., Bell, G., Hopkins, F., Kitidis, V., Cazenave1, P., Nightingale, P., Yelland, M., Pascal, R.,

5   Prytherch, J., Brooks, I., and Smyth, T.: Air–sea fluxes of CO_2 and CH_4 from the Penlee Point Atmospheric Observatory on the south-west coast of the UK, Atmospheric Chemistry and Physics, 16, 5745-5761, 2016.

Wagner-Riddle, C., Congreves, K. A., Abalos, D., Berg, A. A., Brown, S. E., Ambadan, J. T., Gao, X.

10   and Tenuta, M.: Globally important nitrous oxide emissions from croplands induced by freeze–thaw cycles, Nature Geoscience, doi:10.1038/ngeo2907, 2017

Wagner-Riddle, C., Furon, A., McLaughlin, N. L., Lee, I., Barbeau, J., Jayasundara, S., Parkin, G., von Bertoldi, P., and Warland, J. S.: Intensive management of nitrous oxide emissions from a corn-soybean-

15   winter-wheat rotation under two contrasting management systems over 5 years, Global Change Biology, 13, 1722-1736, 2007.

Wagner-Riddle, C., Thurtell, G., and Edwards, G.: Micrometeorology in Agricultural Systems, chapter Trace Gas Concentration Measurements for Micrometeorological Flux Quantification, American

20   Society of Agronomy, Crop Science Society of America, Soil Science Society of America, 321-343, 2005.

Wang, D., Wang, K., Díaz-Pinés, E., Zheng, X., and Butterbach-Bahl, K.: Applicability of an eddy covariance system based on a close-path quantum cascade laser spectrometer for measuring nitrous

25   oxide fluxes from subtropical vegetable fields, Atmospheric and Oceanic Science Letters, 9, 5, 381-387, 2016.

Webb, E. K., Pearman, G. I., Leuning, R.: Correction of flux measurements for density effects due to heat and water vapour transfer, Q J R Meteorol Soc, 106, 85-100, 1980.

Table 1: Sampling system details for each analyzer throughout the measurement campaign. Changes to equipment during the experimental period are indicated. Operating configurations of N_2O analyzers used in Rannik et al. (2015) are given for comparison.

	Filter	Dryer	Pump	Flow (L min^{-1})	Cell Pressure (mb)	Cell Volume (mL)	Tube ID (mm)	Tube Length (m)
Current study								
TDLAS-LN								
before 8 Jul 2015	2 µm^{pp}	multi-tube	rotary vane	14.5	58	480	4.3	6
after 8 Jul 2015	2 µm^{pp}	multi-tube	rotary vane	14.5	58		4.3	10
TDLAS-TE								
before Jun 2015	2 µm^{pp}	multi-tube	rotary vane	14.5	59	200	4.3	6
after 24 Jun 2015	vortex	single tube	scroll	3.5	32		2.2	9.1
EC155								
before Feb 2016	20 µm^{ss}	none	diaphragm	7	950	6	2.7	0.6
after 4 Feb 2016	vortex			6	910		2.2	0.6
From Rannik et al. (2015)								
TGA100A (Campbell Scientific Inc.)				17	50	480	4	17.8
CW-TILDAS-CS (Aerodyne Research Inc.)				13.2	53	500	4	16
N2O/CO-23d (Los Gatos Research Inc.)				11.6	117	408*	8	16
QC-TILDAS76-CS (Aerodyne Research Inc.)				13.5	53	500	4	8.5

*from LGR user manual

Notes:

pp – polypropylene

ss – stainless steel

Table 2: Analyzer frequency response characteristics from this study and that of Rannik et al., (2015). Residence times (τ_{res}) were calculated from values given in Table 1. $f_{c,t}$ is the theoretical best-case cutoff frequency, assuming no mixing for the single-pass sample cells and complete mixing for the multi-pass sample cells, and $\tau_{e,t}$ is the corresponding effective time constant. f_c and τ_e are results from the impulse response test. Results ($\tau_{e,s}$ and $f_{c,s}$) from Rannik et al. (2015) were derived from cospectral analyses. The tube delays t_{del} are the measured total delay minus the processing delay. Time constants and t_{del} are in units of ms and cutoff frequencies are in Hz.

	τ_{res}	$f_{c,t}$	$\tau_{e,t}$	f_c	τ_e	t_{del}
Current study:						
TDLAS-LN	114	3.88	41	2.30	69	720
TDLAS-TE	48	9.22	17	—	—	—
TDLAS-TE (vortex)	108	4.10	39	3.50	48	578
EC155	54	8.19	19	4.05	39	100
From Rannik et al., 2015:				$f_{c,s}$	$\tau_{e,s}$	
TGA100A (Campbell Scientific Inc.)	100*	4.42	36	1.33	120	—
CW-TILDAS-CS (Aerodyne Research Inc.)	119	1.34	119	2.27	70	—
N2O/CO-23d (Los Gatos Research Inc.)	244	0.65	244	0.61	260	—
QC-TILDAS76-CS (Aerodyne Research Inc.)	116	1.37	116	1.99/0.94[†]	80/150[†]	—

*Assumes 15% of flow is used for purge.
[†]Calculated with CO_2
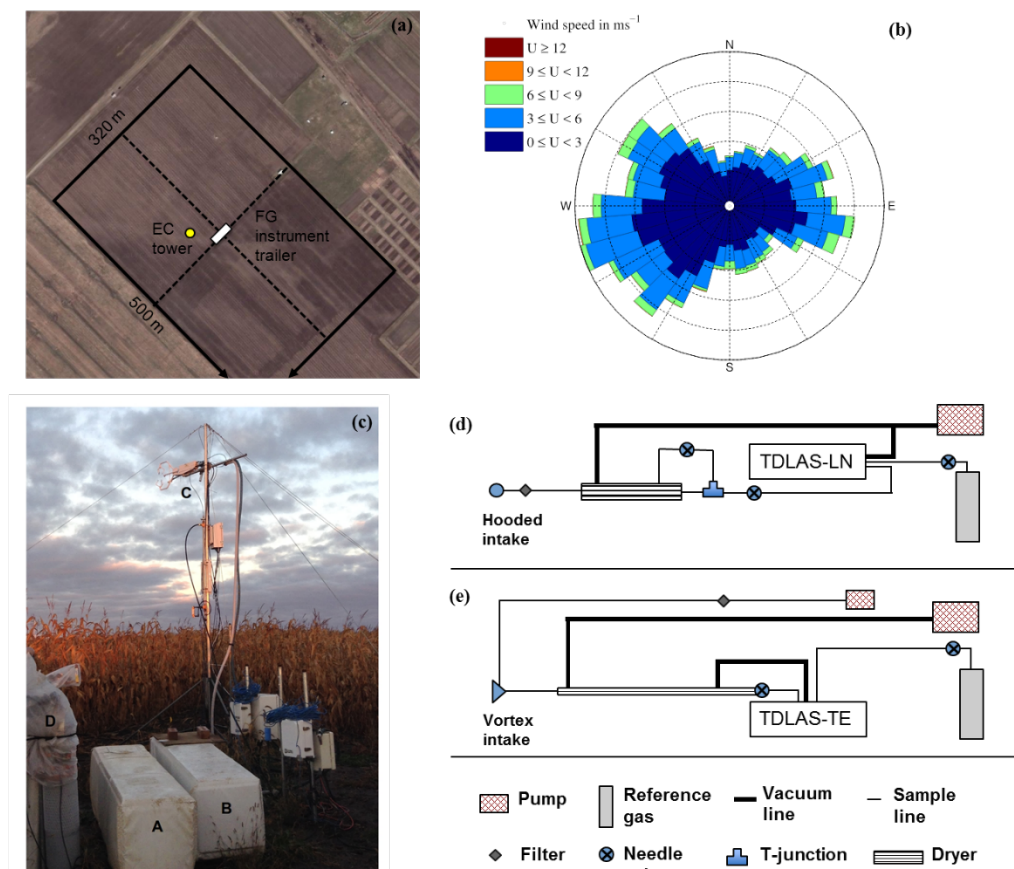
Figure 1: Descriptions of the field site and eddy covariance instrumentation. (a) Layout of the field site. Dashed lines indicate the borders of the field treatments used in the larger 4-plot flux gradient (FG) study. Instrumentation for that study was housed in the indicated instrumentation trailer located in the center of the field. Solid lines outline the entire field. (b) Wind rose of the wind speeds and direction observed during the field study. (c) Configuration of the analyzers at the EC tower; A – TDLAS-LN, B – TDLAS-TE, C – EC155, D - reference gases for the N_2O analyzers. (d) schematic of TDLAS-LN sampling system with inline filter and multi-tube dryer. (e) schematic of TDLAS-TE sampling system with vortex intake and single-tube dryer.
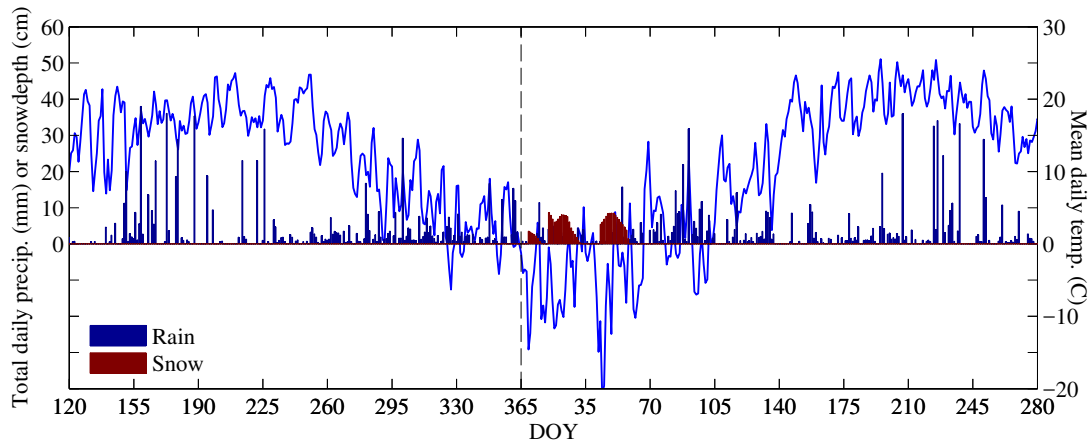
Figure 2: Daily precipitation and temperature for 2015 and 2016. Rain values (mm) are the total rainfall per day, snow values (cm) are the depth of snow present.
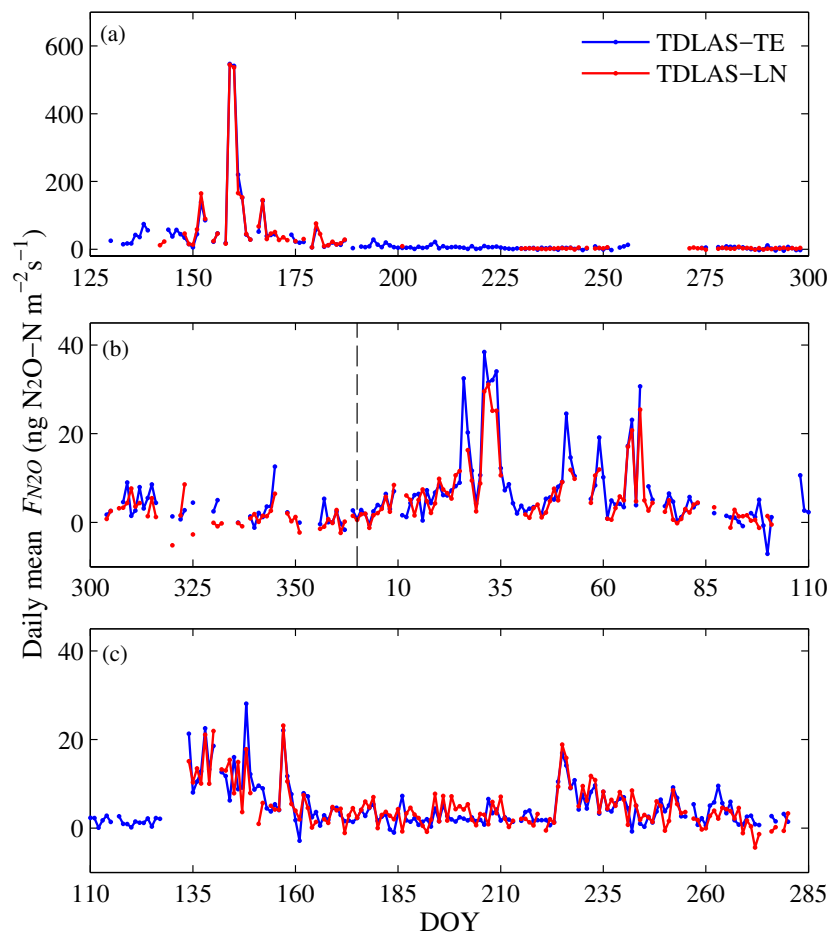
Figure 3: Mean daily fluxes of N_2O-N measured by each analyzer. Figure (a) shows the period of high N_2O fluxes in the post-fertilization period of 2015 and the fluxes measured throughout the growing season. Figure (b) shows the fluxes measured during the post-harvest period of 2015 and winter of 2016. The dotted line in (b) demarcates the separation between years 2015 and 2016. Figure (c) shows fluxes measured from early spring to the end of the growing season of 2016.
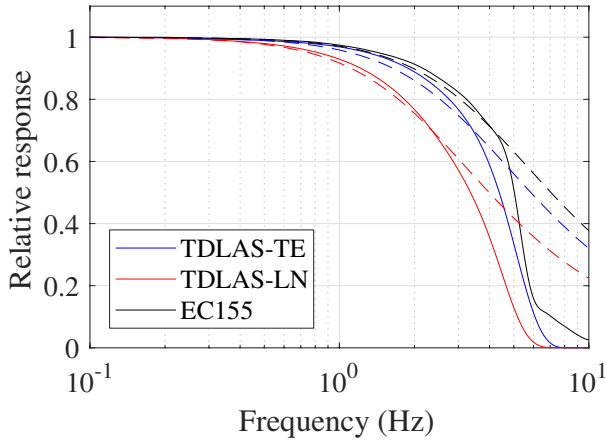
Figure 4: Results of the frequency response test of TDLAS-LN and TDLAS-TE for N_2O and the EC155 (CO_2) under normal operating conditions (solid lines), dashed lines are modeled T_{FR} calculated using the measured f_c in equation 1.
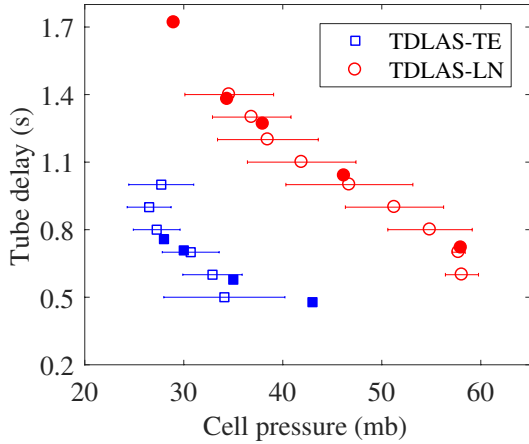
Figure 5: Tube delay (t_{del}) determined from the frequency response test (solid symbols) and from the cross-correlation between the CO_2 and w (open symbols) across the range of operating pressures. Error bars are the standard deviation of the mean cell pressure associated with each value.
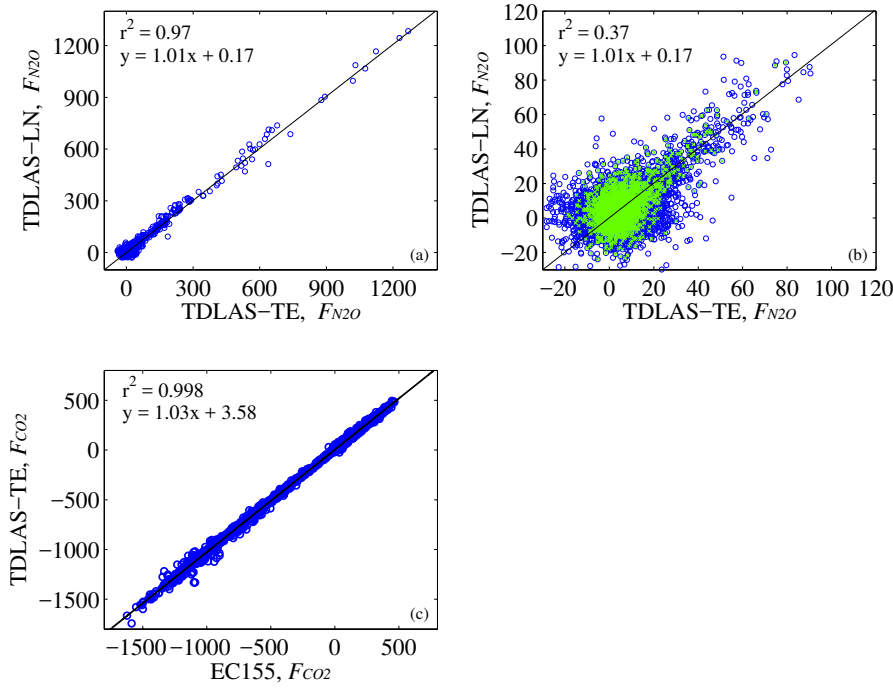
Figure 6: Comparison of 30 min fluxes measured by each analyzer. Figure (a) displays the comparison of N_2O-N fluxes (ng N_2O-N m^{-2}s^{-1}) for the entire dataset, (b) shows the same N_2O-N flux dataset (ng N_2O-N m^{-2}s^{-1}) but centered on the low flux values. The green 'x' markers in Figure (b) are the fluxes measured when the standard deviation of background N_2O concentrations for both analyzers was less than 2 ppb N_2O. Figure (c) is the comparison of F_{CO2} between TDLAS-TE and EC155 (μg CO_2 m^{-2}s^{-1}).
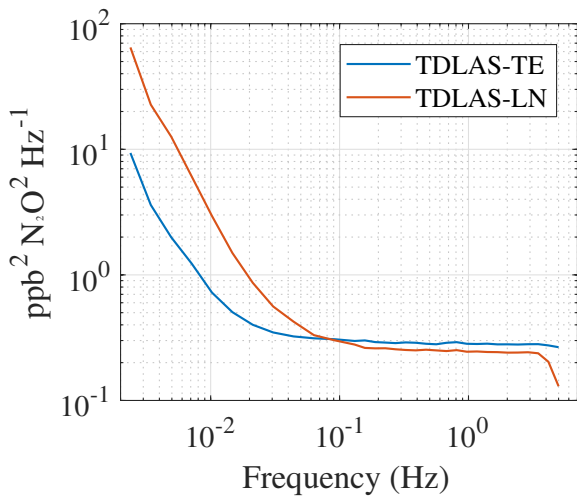
Figure 7: Mean N_2O variance spectra of each TDLAS analyzer from 29 June 2016 to 9 July 2016.
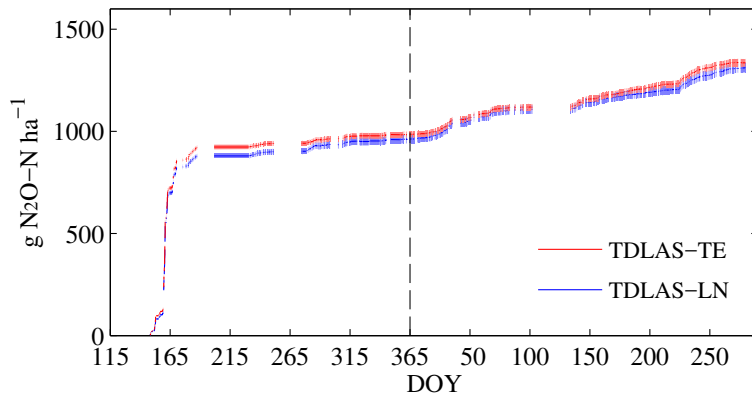
Figure 8: Cumulative N_2O-N emissions. Shaded areas represent the $p = 0.05$ confidence intervals calculated using the random error calculations.